Entangled spin clusters : some special features

Amit Tribedi and Indrani Bose

1st February 2008

Department of Physics

Bose Institute

93/1, Acharya Prafulla Chandra Road

Kolkata - 700 009, India

Abstract

In this paper, we study three specific aspects of entanglement in small spin clusters. We first study the effect of inhomogeneous exchange coupling strengths on the entanglement properties of the S=$\frac{1}{2}$ antiferromagnetic linear chain tetramer compound $NaCuAsO_4$. The entanglement gap temperature, T_E, is found to have a non-monotonic dependence on the value of α, the exchange coupling inhomogeneity parameter. We next determine the variation of T_E as a function of S for a spin dimer, a trimer and a tetrahedron. The temperature T_E is found to increase as a function of S but the scaled entanglement gap temperature t_E goes to zero as S becomes large. Lastly, we study a spin-1 dimer compound to illustrate the quantum complementarity relation. We show that in the experimentally realizable parameter region, magnetization and entanglement plateaus appear simultaneously at low temperatures as a function of the magnetic field. Also, the sharp increase in one quantity as a function of the magnetic field is accompanied by a sharp decrease in the other so that the quantum complementarity relation is not violated.

I. INTRODUCTION

Entanglement is a key feature of quantum mechanical systems and gives rise to non-local correlations over and above those expected from classical considerations [1]. It can be of different types : bipartite, multipartite, zero-temperature, finite-temperature etc. for which suitable measures are available in certain cases [2, 3, 4, 5, 6, 7, 8]. In the past few years, quantum spin systems have been extensively studied to gain knowledge on the different aspects of entanglement. The spins in such systems interact via the exchange interaction and also with an external field, if any. Several studies show that the amount

of entanglement can be changed by varying the temperature T and/or the magnitude of the external field [3, 4, 9]. In the case of entangled thermal states, one can define a critical temperature below which entanglement is present in the system and above which entanglement vanishes, i.e., the system becomes separable. Detection of entanglement can be made with the help of an entanglement witness (EW) which is an observable the expectation value of which is positive in separable and negative in entangled states [10, 11, 12]. Thermodynamic observables like internal energy, magnetization and susceptibility have been proposed as EWs [12, 13, 14]. There is now experimental evidence that entanglement can affect the macroscopic properties of solids like specific heat and magnetic susceptibility [15]. Recently, it has been shown that for separable states, the sum of magnetic susceptibilities in the three orthogonal directions x, y, and z obeys the inequality

$$\bar{\chi} \equiv \chi_x + \chi_y + \chi_z \geq \frac{N\,S}{k_B T} \tag{1}$$

where N is the total number of spins in the system, S the magnitude of the spin, k_B the Boltzmann constant and T the temperature [14]. If the magnetization operator $M_\alpha = \sum_j S_j^\alpha$ commutes with the Hamiltonian H of the system, i.e., $[H, M_\alpha] = 0$, the magnetic susceptibility χ_α (α =x, y, z) can be written as

$$\chi_\alpha = \frac{1}{k_B T}\left[\left\langle (M_\alpha)^2 \right\rangle - \langle M_\alpha \rangle^2\right] \tag{2}$$

$$= \frac{1}{k_B T}\left[\sum_{i,j=1}^{N} \left\langle S_i^\alpha S_j^\alpha \right\rangle - \left\langle \sum_{i=1}^{N} S_i^\alpha \right\rangle^2\right] \tag{3}$$

Thermodynamic properties in general relate to macroscopic systems and the thermal state of such a system is entangled if $\bar{\chi}$ is $< \frac{N\,S}{k_B T}$ (Eq. (1)). Using the susceptibility inequality as an EW, one can detect entanglement from the experimental data without requiring a knowledge of the Hamiltonian of the system.

For a multipartite Hamiltonian H, one can define the entanglement gap as

$$G_E = E_{sep} - E_g \tag{4}$$

where E_{sep} is the minimum separable energy and E_g the ground state energy of the Hamiltonian [12]. For a spin Hamiltonian, E_{sep} is the ground state energy of the equivalent classical Hamiltonian [11]. If a system has entanglement gap $G_E > 0$, then one can define the entanglement gap temperature, T_E, as the temperature at which the thermal (internal) energy $U(T_E) = E_{sep}$. For temperature $T < T_E$, the thermal state of the system is bound to be entangled. Recently, a quantum complementarity relation has been proposed [14] between the thermodynamic observables, magnetization and magnetic susceptibility. This is given by

$$1 - \frac{k_B T \bar{\chi}}{N\,S} + \frac{\left\langle \vec{M} \right\rangle^2}{N^2 S^2} \leq 1 \tag{5}$$

where $\left\langle \overrightarrow{M} \right\rangle^2 \equiv \langle M_x \rangle^2 + \langle M_y \rangle^2 + \langle M_z \rangle^2$. Define the quantities

$$P = \frac{\left\langle \overrightarrow{M} \right\rangle^2}{N^2 S^2} \ , \ Q = 1 - \frac{k_B T \bar{\chi}}{N\, S} \tag{6}$$

The quantity P, which depends upon the magnetization, describes the local properties of individual spins whereas Q, which involves the susceptibility, is representative of quantum spin-spin correlations. From Eq. (1), a nonzero positive value of Q implies the presence of entanglement in the system, i.e., non-local correlations. The complementarity relation shows that the non-local properties are enhanced at the expense of the local properties in order that $P + Q$ is ≤ 1.

The EWs based on the internal energy and susceptibility have been used to study the entanglement properties of the spin-$\frac{1}{2}$ antiferromagnetic (AFM) compounds $Cu(NO_3)_2, 2.5D_2O(CN)$(system of weakly coupled spin dimers) [13], $(NHEt)_3 \left[V_8^{IV} V_4^V As_8 O_{40} (H_2O)\right].H_2O$ (system of weakly coupled spin tetramers) [16] and the nanotubular system $Na_2V_3O_7$ (consists of weakly-coupled nine-spin rings) [17]. The weak coupling between the spin clusters allows each system to be treated as consisting of effectively independent clusters. Since the clusters contain a few spins, the theoretical calculation of entanglement-related quantities becomes possible. A number of molecular magnets are known which are well-described in terms of small spin clusters such as dimers, trimers, tetramers, tetrahedra etc [18]. For non-bipartite clusters with "all-to-all" spin couplings (trimers, tetrahedra), the EWs based on the internal energy and susceptibility give the same estimate of the temperature above which entanglement vanishes [16]. For bipartite clusters (a tetramer describing a square plaquette of spins with only nearest-neighbour(NN) exchange couplings provides an example), the EW based on the internal energy can detect only the bipartite entanglement between two qubits [12]. The spin clusters considered so far are described by Hamiltonians with homogeneous exchange interaction strengths. In this paper, we consider the $S = \frac{1}{2}$ AFM linear tetramer compound $NaCuAsO_4$ [19] in which the linear tetramer consisting of four spins is described by the Heisenberg Hamiltonian

$$H_{LT} = J\, \overrightarrow{S_1}.\overrightarrow{S_2} + \alpha J\, \overrightarrow{S_2}.\overrightarrow{S_3} + J\, \overrightarrow{S_3}.\overrightarrow{S_4} \tag{7}$$

We study the entanglement properties of this compound using both the internal energy and the susceptibility as EWs. We next determine the entanglement gap temperature T_E of small spin clusters as a function of the magnitude S of spins. Lastly, we determine the quantities P and Q (Eq. (6)) appearing in the complementarity relation (Eq. (5)) for a spin-1 dimer compound $[Ni_2\,(Medpt)_2(\mu{-}ox)(H_2O)_2](ClO_4)_2.2H_2O$ [20] and show that the sharp changes in the magnetization and the formation of plateaus at low temperatures are accompanied by sharp changes and plateaus in the amount of entanglement. Magnetization plateaus have been observed experimentally in the spin-1 dimer compound. This compound thus provides a concrete example of a system in which the amount of entanglement can change steeply as a function of the magnetic field or does not change over a range of field values.

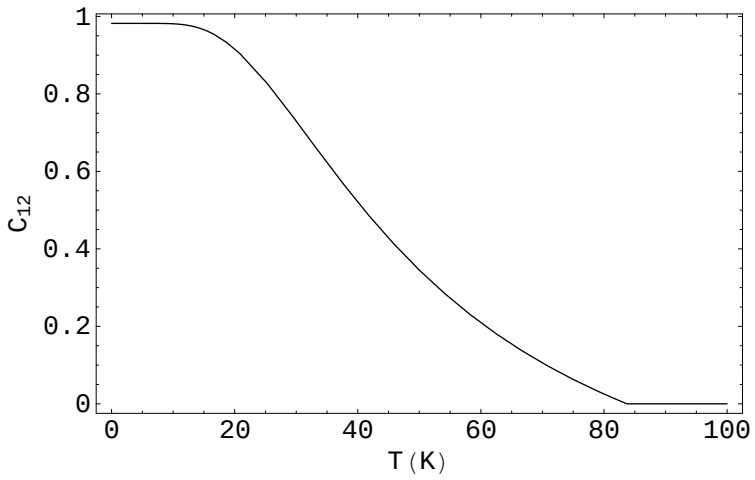

FIG. 1. Concurrence C_{12} as a function of temperature for $\alpha = 0.4$ and $\frac{J}{k_b} = 92.7K$.

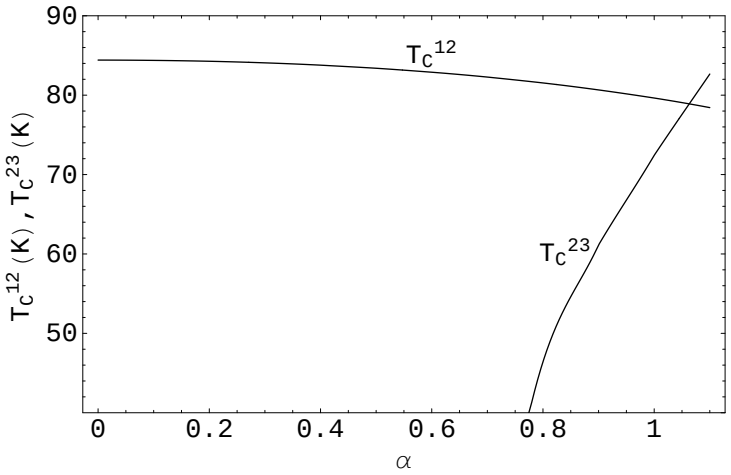

FIG. 2. Plots of T_C^{12} and T_C^{23} versus α. T_C^{kl} is the critical entanglement temperature for the pair of spins at sites k and l.

II. LINEAR CHAIN TETRAMER

The $S = \frac{1}{2}$ AFM compound $NaCuAsO_4$ has a linear chain tetrameric structure described by the Hamiltonian, H_{LT}, in Eq. (7) with $\alpha \approx 0.4$. The term "linear" refers to the pattern of exchange couplings and not to the spatial structure of the tetramer [19]. The total spin S^{tot} of the tetramer has the values 2, 1 and 0. There are five $S^{tot} = 2$ states, nine $S^{tot} = 1$ states and two $S^{tot} = 0$ states. The different eigenvalues and eigenvectors are displayed in Appendix A. We now discuss the finite-temperature entanglement properties of the linear chain tetramer. The thermal density matrix $\rho(T)$ is given by

$$\rho(T) = \frac{1}{Z} \sum_{E_i} \sum_{m} e^{-\beta E_i} |\psi_{i,m}\rangle \langle\psi_{i,m}| \tag{8}$$

The first summation is over all the independent energy eigenstates and the second summation includes terms corresponding to the $(2S^{tot} + 1)$ degenerate eigenstates with the eigenvalue E_i. Z denotes the partition function

$$Z = \sum_{E_i} \left(2S^{tot} + 1\right) e^{-\beta E_i} \tag{9}$$

A measure of entanglement between the spins at sites k and l is given by the concurrence C_{kl}. This is calculated from the reduced thermal density matrix $\rho_{kl}(T)$ using standard procedure [2, 9]. Since the eigenvalues and eigenvectors of the linear chain tetramer are known, the calculation of C_{kl} is straightforward. Figure 1 shows the variation of C_{12} as a function of temperature for $\alpha = 0.4$ and $\frac{J}{k_B} = 92.7\,K$, the parameter values relevant for $NaCuAsO_4$ [18, 19]. The concurrence C_{23} is zero for these parameter values. One can further define a critical temperature T_C^{kl} above which the entanglement between the spins at the sites k and l disappears. Figure 2 shows a plot of T_C^{12} and T_C^{23} versus α for $\frac{J}{k_B} = 92.7K$. We next calculate the entanglement gap temperature T_E at which the internal energy

$$U(T_E) = -\frac{1}{Z}\left(\frac{\partial Z}{\partial \beta}\right) = E_{sep} \tag{10}$$

where E_{sep} is the minimum separable energy. Figure 3 shows a plot of T_E versus α for $\frac{J}{k_B} = 92.7K$ (Curve a). The operator $H - E_{sep}$ is an EW since $Tr\left[\rho\left(H - E_{sep}\right)\right] = U(T) - E_{sep}$ is < 0 (≥ 0) when the thermal state is entangled (separable). If the Hamiltonian H of the system contains only local interactions such that $H = \sum_{<ij>} H_{ij}$ and the underlying lattice is bipartite, then

$$H - E_{sep} = \sum_{<ij>} \left(H_{ij} - e_{sep,ij}\right) \tag{11}$$

where $e_{sep,ij}$ is the minimum separable energy associated with the interaction between the spins located at the sites i and j. In the case of a translationally invariant Hamiltonian, H_{ij} and $e_{sep,ij}$ are the same for each interacting spin pair. Each term in the sum on the RHS of Eq. (11) can be considered as a bipartite EW. Thus the expectation value of

$H - E_{sep}$ is negative only if the two spins in the interacting spin pairs are entangled. In the case of the linear chain tetramer, the Hamiltonian H_{LT} is not translationally invariant. This is true even in the limit $\alpha = 1$. Since, the H_{ij}'s and $e_{sep,ij}$'s are no longer the same for each interaction bond, $T_C^{12} = T_C^{34} \neq T_C^{23}$. The expectation value of $H - E_{sep}$ now depends on the relative magnitudes and signs of the two types of terms on the RHS of Eq. (11). In contrast, consider a closed chain of four spins in which the NN spins interact with the same exchange interaction strength. In this case, because of translational invariance, $T_C^{12} = T_C^{23} = T_C^{34} = T_C^{41} = T_C$ and the entanglement gap temperature T_E is equal to T_C, the critical temperature beyond which the entanglement between two NN spins vanishes (concurrence is zero). In the case of the linear chain tetramer, a similar interpretation cannot be given.

We now use the magnetic susceptibility as an EW to determine the critical temperature T_C^{χ} beyond which the thermal state of the linear chain tetramer is separable. We consider the case of zero-field susceptibility. In the absence of a magnetic field, $\langle M_\alpha \rangle = 0\,(\alpha = x, y, z)$. Also, due to the spin isotropy of the Hamiltonian, H_{LT}, (S^{tot} is a good quantum number), $\chi_x = \chi_y = \chi_z = \chi$. The susceptibility χ can be written as

$$\chi = \frac{\beta}{3Z} \sum_{E_i} \left(2S^{tot} + 1\right) \left(S^{tot} + 1\right) S^{tot} e^{-\beta E_i} \tag{12}$$

The susceptibility inequality for separable states (Eq. (1)) becomes

$$\chi \geq \frac{NS}{3k_B T} \tag{13}$$

The critical temperature T_C^{χ} is given by the intersection point of the two curves : χ versus T plot from Eq. (12) and χ versus T plot from the equality in Eq. (13) [14, 16]. For $\alpha = 0.4$ and $\frac{J}{k_B} = 92.7\,K$, one obtains the estimate $T_C^{\chi} = 90.88\,K$, which is really the lower bound of the critical temperature above which entanglement vanishes. Figure 3 also shows the variation of T_C^{χ} as a function of α (Curve b). Since the linear chain tetramer is associated with a bipartite graph, T_C^{χ} is $> T_E$, the entanglement gap temperature.

III. GENERAL SPIN S AND T_E

We have so far considered the case $S = \frac{1}{2}$. We now consider dimers, trimers and tetrahedra of spins of magnitude S. The Hamiltonians describing the small clusters are

$$H_{dimer} = J\, \overrightarrow{S_1}.\overrightarrow{S_2} \tag{14}$$

$$H_{trimer} = J\, \left(\overrightarrow{S_1}.\overrightarrow{S_2} + \overrightarrow{S_2}.\overrightarrow{S_3} + \overrightarrow{S_3}.\overrightarrow{S_1}\right) \tag{15}$$

$$H_{tetrahedron} = J\, \left(\overrightarrow{S_1}.\overrightarrow{S_2} + \overrightarrow{S_2}.\overrightarrow{S_3} + \overrightarrow{S_3}.\overrightarrow{S_4} + \overrightarrow{S_4}.\overrightarrow{S_1} + \overrightarrow{S_1}.\overrightarrow{S_3} + \overrightarrow{S_2}.\overrightarrow{S_4}\right) \tag{16}$$

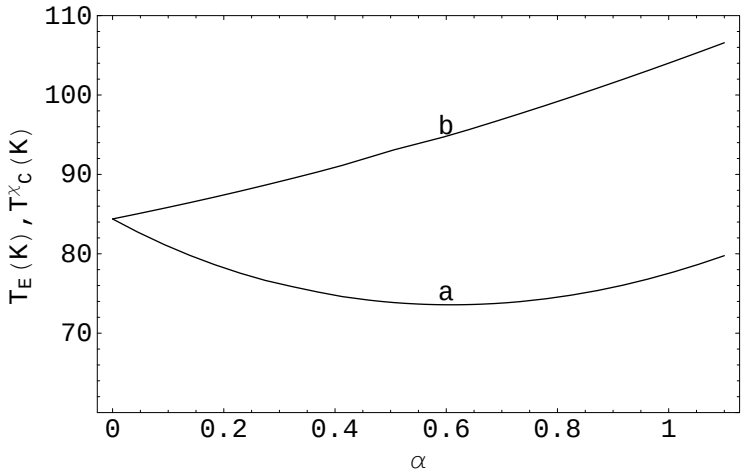

FIG. 3. Plots of T_E (Curve a) and T_C^{χ} (Curve b) for the linear chain tetramer as a function of α ($\frac{J}{k_B} = 92.7\,K$).

A trimer and a tetrahedron are defined on a non-bipartite graph. The AFM cluster Hamiltonian in each case contains "all-to-all" spin couplings and is frustrated as there is no separable state that simultaneously minimizes the energy of each interacting spin pair. Thus $e_{sep,ij}$ in Eq. (11) is no longer the minimum separable energy of an interacting spin pair, it has a magnitude greater than that of the latter quantity. The minimum separable energy for the whole Hamiltonian is $E_{sep} = \sum_{<ij>} e_{sep,ij} = N_{tot}\, e_{sep}$, where N_{tot} is the total number of interacting spin pairs. Since e_{sep} is greater than the minimum separable energy for an interacting spin pair, the EW, $H - E_{sep}$, can detect entanglement even if the entanglement between the spins in the interacting spin pair vanishes, i.e., the corresponding reduced density matrix becomes separable [12]. In this case, the entanglement gap temperature T_E is T_C, the critical temperature beyond which the NN concurrence is zero. As shown in [16], $T_E = T_C^{\chi}$ for $S = \frac{1}{2}$ non-bipartite clusters like the trimer and the tetrahedron described by the Heisenberg Hamiltonian with homogenous exchange couplings. This result holds true for general S in the case of spin clusters with "all-to-all" homogeneous Heisenberg spin couplings. We thus use only the internal energy-based EW to determine how the critical entanglement temperature varies as a function of S in the cases of the spin dimer, trimer and the tetrahedron.

For Hamiltonians with "all-to-all" spin couplings, the energy eigenvalues of all the eigenstates can be determined quite easily from a simple formula. The Hamiltonian can be written as

$$H = \frac{1}{2}\left[\left(\overrightarrow{S}^{tot}\right)^2 - \sum_{i=1}^{N} S_i^2\right] \tag{17}$$

where $\overrightarrow{S}^{tot} = \sum_{i=1}^{N} \overrightarrow{S}_i$. The eigenvalue $E_{S^{tot}}$ for a state with total spin S^{tot} is

$$E_{S^{tot}} = \frac{1}{2}\left[S^{tot}\left(S^{tot}+1\right) - NS\left(S+1\right)\right] \tag{18}$$

where S is the magnitude of a spin. The possible values of S^{tot} are NS, $NS-1$, ...etc. The lowest value is zero for N even and $\frac{1}{2}$ for N odd. Under the vector addition of angular momenta, a particular S^{tot} value can be achieved in more than one way, i.e., has some multiplicity. Let $P^S_{S^{tot}N}$ be the multiplicity, i.e., the number of possible states with total spin angular momentum S^{tot} when N spins, each of magnitude S, are combined. As shown by Mikhailov [21], $P^S_{S^{tot}N}$ is given by

$$P^S_{S^{tot}N} = \sum_k (-1)^k \begin{pmatrix} N \\ k \end{pmatrix} \begin{pmatrix} N(S+1) - S^{tot} - (2S+1)k - 2 \\ N-2 \end{pmatrix} \tag{19}$$

Here $\begin{pmatrix} m \\ n \end{pmatrix}$ are the binomial coefficients. The summation index k satisfies two conditions : $(i)\, k \geq 0$ and (ii) the upper numbers in the binomial coefficients cannot be less than the lower numbers. Thus, $0 \leq k \leq [\frac{(SN-S^{tot})}{2S+1}]$ where $[b]$ denotes the integer part of b. The minimum separable energy of a spin cluster is equal to the ground state energy of the equivalent classical Hamiltonian. In the classical ground state, $S^{tot} = 0$ and each $< S_i^2 >= S^2$. Thus, the minimum separable energy, E_{sep}, for the dimer, trimer and tetrahedron is given by $E_{sep} = -S^2$(dimer), $-\left(\frac{3}{2}S^2\right)$ (trimer) and $-2S^2$(tetrahedron). The entanglement gap temperature T_E can be calculated by using the relation in Eq. (10). Figure 4 shows the variation of T_E with S for dimers (star), trimers (solid square) and tetrahedra (solid diamond). The entanglement gap temperature, T_E, is found to increase with S in each case. According to conventional notion, spins behave as classical objects in the limit of large S. The commutation bracket of spin operators, with each operator scaled by the total spin S, tends to zero as $S \to \infty$. One would thus expect the entanglement gap temperature T_E to decrease rather than increase as the magnitude of S is raised. Some earlier studies have reported findings similar to ours. Hao and Zhu [22] have studied the AFM Heisenberg chain with spins of magnitude S. For a two-sited chain, i.e., a dimer, they find that the entanglement gap temperature T_E increases almost linearly with S. For $S = 1$, they have shown that T_E decreases as the length of the chain is increased. Wieśniak et al. [14] have determined the critical entanglement temperature, T_C^χ, based on the susceptibility as an EW, and find the result that $T_C^\chi = 1.6\,J$ for the $S = \frac{1}{2}$ Heisenberg chain and $T_C^\chi = 2\,J$ for a chain of spins 1. As pointed out by Dowling et al. [12], it is sensible to define a scaled temperature

$$t = \frac{k_B T}{E_{tot}} \tag{20}$$

for a meaningful comparison of Hamiltonians with different total energy ranges, E_{tot} (E_{tot} is the difference between the highest and the lowest energy eigenvalues). The scaled entanglement gap temperature can be defined as $t_E = \frac{k_B T_E}{E_{tot}}$. The inset of Fig. 4 shows the variation of t_E with S for dimers (star), trimers (solid triangle) and tetrahedra (solid

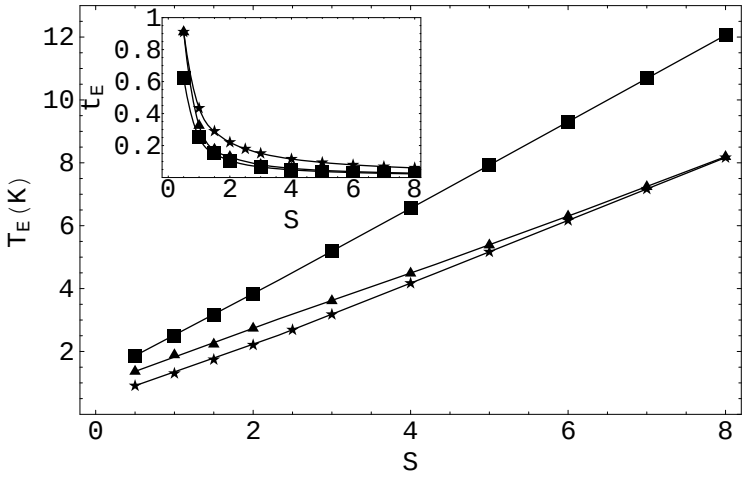

FIG. 4. Variation of the entanglement gap temperature, T_E, with S for dimers (star), trimers (solid triangle) and tetrahedra (solid square). The inset shows the variation of the scaled entanglement gap temperature t_E with S.

square). One finds that the scaled entanglement gap temperature decreases as S increases. The result can be interpreted in the following way. As S increases, the fraction of the total energy range of the spin system which corresponds to entangled states decreases and tends to a limiting value as $S \to \infty$. Classical behaviour presumably emerges when the entangled states have a negligible contribution to the total energy range.

IV. SPIN-1 DIMER : QUANTUM COMPLEMENTARITY

Bose and Chattopadhyay [23] have considered some toy spin models and shown that first order quantum phase transitions, occurring at special values of the external magnetic field, are accompanied by magnetization and entanglement jumps. Upward jumps in the magnetization give rise to downward jumps in the amount of entanglement. Also, magnetization and entanglement plateaus coexist in the same range of magnetic fields. Later studies established the general validity of these results [24, 25, 26]. In this section, we show that the quantum complementarity relation (Eq. (5)) provides a natural explanation for the correlated changes in the amounts of magnetization and entanglement as a function of the magnetic field. We illustrate this in the case of a spin-1 dimer compound $[Ni_2\,(Medpt)_2(\mu-ox)(H_2O)_2](ClO_4)_2.2H_2O$ $(Medpt = methyl-bis(3-aminopropyl)amine)$ which exhibits magnetization plateaus at sufficiently low temperatures [20]. The Hamiltonian describing the spin-1 dimer is

$$H_d = J\,(S_1^x S_2^x + S_1^y S_2^y) + \delta J\,(S_1^z S_2^z) + d\left[(S_1^z)^2 + (S_2^z)^2\right] + B\,(S_1^z + S_2^z) \qquad (21)$$

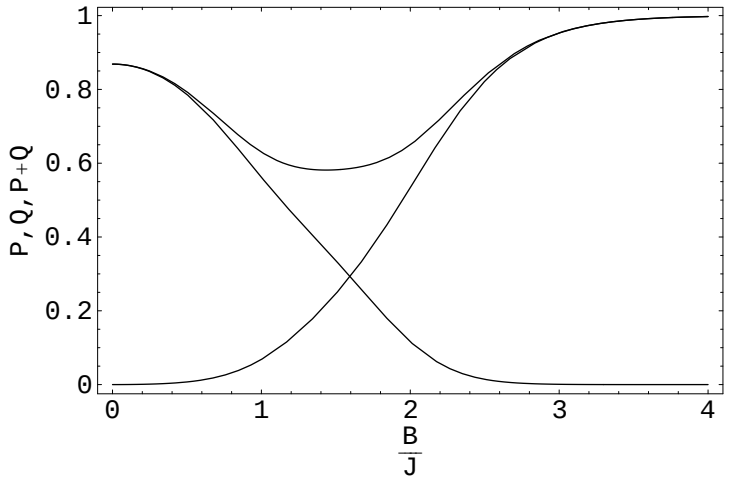

FIG. 5. Plots of P, Q and $P+Q$ as a function of $\frac{B}{J}$ in the case of a spin-1 dimer ($\delta = 1$, $d = 0$ and $\beta J = 3$.)

where δ is the exchange anisotropy parameter, d labels the axial zero-field splitting parameter and B the strength of the external magnetic field. The negative (positive) sign of the parameter d corresponds to an easy-axis (easy-plane) single ion anisotropy. If the spin system is entangled, a sharp increase in the magnetization (obtained at low temperatures) is accompanied by a sharp decrease in the amount of entanglement so that the complementarity relation is not violated. At $T = 0$, the sharp changes become the 'jumps' associated with first order quantum phase transitions. As T increases, the changes occur more gradually as a function of the magnetic field. In an entangled system, the magnetization plateaus are accompanied by entanglement plateaus and the complementarity relation continues to be valid. To illustrate this, we first calculate the eigenvalues and the eigenvectors of the dimer Hamiltonian H_d (Eq. (37)). These are displayed in Appendix B. The magnetization M (only the z-component is non-zero) and χ_z, the z-component of the susceptibility are derived from

$$M = \frac{1}{\beta Z}\frac{\partial Z}{\partial \beta},\ \chi_z = \frac{\partial M}{\partial B} \tag{22}$$

The susceptibility components χ_x and χ_y are determined from Eq. (3) with $\langle S_1^x \rangle$, $\langle S_1^y \rangle$, $\langle S_2^x \rangle$ and $\langle S_2^y \rangle = 0$ since the magnetic field is in the z-direction. One can now calculate the terms P and Q (Eq. (6)) appearing in the quantum complementarity relation given by Eq. (5).

Figure 5 shows the plots of P, Q and $P+Q$ as a function of $\frac{B}{J}$ for $\delta = 1$, $d = 0$ and $\beta J = 3$. Figure 6 shows the appearance of plateaus as the temperature is lowered ($\beta J = 20$). Note that a sharp increase in P is accompanied by a sharp decrease in Q. Plateaus in P and Q occur in the same range of magnetic fields. At sufficiently low temperatures, the two-step plateau structure is still obtained for non-zero values of d. The intermediate plateau has a lesser width for negative values of d and disappears at $d = -1$. At this point, Q is ≤ 0 throughout the range of $\frac{B}{J}$ values so that the spin system is not

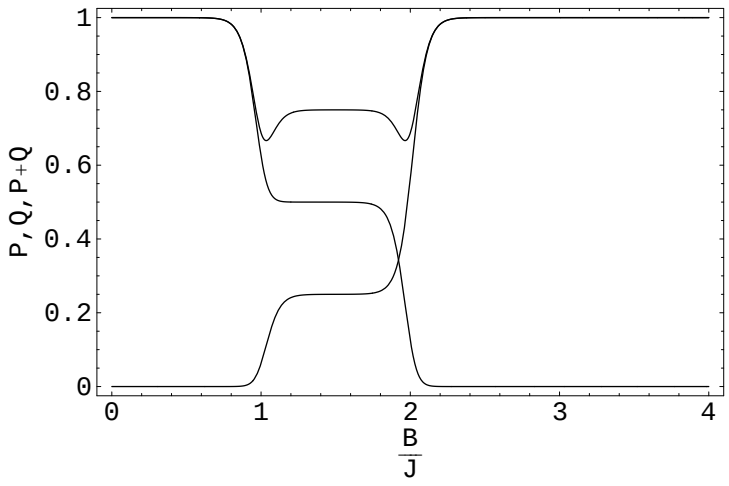

FIG. 6. Plots of P, Q and $P+Q$ as a function of $\frac{B}{J}$ in the case of a spin-1 dimer ($\delta = 1$, $d = 0$ and $\beta J = 20$.)

entangled. If d is changed from $d = -1$ to $d = +1$, the two-step structure in both P and Q is recovered and the amount of entanglement is no longer zero. The easy-plane single ion anisotropy ($d > 0$) is found to be favourable towards plateau formation in both P and Q. The changes in P and Q are correlated so that the complementarity relation $P + Q \leq 1$ is always valid. A two-step magnetization curve has been experimentally observed in the spin-1 nickel compound mentioned earlier [20]. Theoretical calculations, based on a description of the compound as a collection of independent spin-1 dimers, give a good fit to the experimental data on the magnetization and susceptibility. The exchange anisotropy parameter δ has been taken as 1 and the single ion anisotropy is of the easy-axis type ($d < 0$). Magnetization experiments have been carried out for the external magnetic field parallel to the z and x directions. In both the cases, a two-plateau structure has been seen in the magnetization versus field curves. In the latter case, the plateau structure is found to be more prominent. Our theoretical calculations suggest that the magnetization plateaus exhibited by the spin-1 nickel compound are accompanied by entanglement plateaus.

V. SUMMARY AND DISCUSSION

In this paper, we study some special features of entangled small spin clusters. We first consider the $S = \frac{1}{2}$ AFM linear chain tetramer compound, $NaCuAsO_4$, described by the Heisenberg exchange interaction Hamiltonian with inhomogeneous exchange coupling strengths (Eq. (7)) and show that the entanglement gap temperature, T_E, has a non-monotonic dependence on the exchange coupling inhomogeneity parameter α. The critical entanglement temperature, T_C^{χ}, obtained by using the susceptibility as an EW, has a monotonic dependence on α. We next determine how the entanglement gap temperature, T_E, varies as a function of S in the cases of small spin clusters like a dimer, a trimer and a

tetrahedron. While T_E increases with S in each case, the scaled entanglement gap temperature t_E decreases as S increases and goes to zero $S \to \infty$. The physical interpretation is that the entangled states have a small contribution to the total energy range in the limit of large S. The general applicability of this result for spin clusters without "all-to-all" spin couplings should be investigated. Tóth [11] has considered a Hamiltonian with "all-to-all" couplings between N spin-$\frac{1}{2}$ particles. The entanglement gap temperature T_E is found to increase as N increases but t_E tends to a constant value as N becomes large. Dowling et al. [12] have given examples of Hamiltonians describing bipartite systems for which t_E increases without bound as the dimension of the Hilbert space associated with the subsystems increases. In our case, with increasing S, the Hilbert space of the system is enlarged but t_E decreases as a function of S and goes to zero in the limit $S \to \infty$. This is so since T_E has a linear variation with S (Fig. 6) and E_{tot} varies as S^2 in the large S limit.

Lastly, we study a spin-1 dimer compound as an illustration of the quantum complementarity relation. In experiments, the compound exhibits low-temperature magnetization plateaus. Our theoretical calculations reproduce these plateaus and further show that if the system is entangled, the magnetization plateaus coexist with the entanglement plateaus. Successive plateaus are connected by sharp changes in the magnetization and the amount of entanglement. The increase in one quantity is compensated by a decrease in the other quantity so that the complementarity relation is not violated. A large number of AFM compounds exhibit the phenomenon of magnetization plateaus [27]. If these systems are entangled at the temperatures for which magnetization plateaus are observed, one can predict the coexistence of magnetization and entanglement plateaus in such systems. The Oshikawa, Yamanaka, Affleck (OYA) [28] theorem provides the condition for the occurrence of magnetization plateaus in quasi-1d AFM systems. Magnetization plateaus have also been observed in a two-dimensional S=$\frac{1}{2}$ AFM system $SrCu_2(BO_3)_2$, thus extending the scope for the applicability of the OYA theorem. It will be of interest to establish a connection between the OYA theorem and the quantum complementarity relation so that the conditions for the simultaneous appearance of the magnetization and the entanglement plateaus are clearly identified.

Acknowledgment. Amit Tribedi is supported by the Council of Scientific and Industrial Research, India under Grant No. 9/15 (306)/ 2004-EMR-I.

References

[1] M. A. Nielsen and I. L. Chuang, Quantum Computation and Quantum Information (Cambridge University Press, Cambridge, 2000)

[2] K. M. O'Connor and W. K. Wootters, Phys. Rev. A 63, 052302 (2001); W. K. Wootters, Phys. Rev. Lett. 80, 2245 (1998)

[3] X. Wang, Phys. Rev. A 64, 012313 (2001); Phys. Lett. A 281, 101 (2001); X. Wang, Phys. Rev. A 66, 034302 (2002)

[4] U. Glasser, H. Büttner and H. Fehske, Phys. Rev. A 68, 032318 (2003)

[5] A. Wong and N. Christensen, Phys. Rev. A 63, 044301 (2001)

[6] C.-S. Yu and H.-S. Song, Phys. Rev. A 73, 022325 (2006)

[7] A. Laxminarayan and V. Subrahmanyam, Phys Rev. A 71, 062334 (2005)

[8] O. Gühne and G. Tóth, quant-ph/0510186, G. Tóth and O. Gühne, Appl. Phys. B 82, 237 (2006).

[9] M. C. Arnesen, S. Bose and V.Vedral, Phys. Rev. Lett. 87,017901 (2001); D. Gunlycke, V. M. Kendon, V. Vedral and S. Bose, Phys. Rev. A 64, 042302 (2001)

[10] M. Lewenstein, B. Kraus, P. Horodecki and J. I. Cirac, Phys. Rev. A 63, 044304 (2001); B. Kraus, M. Lewenstein and J. I. Cirac, Phys. Rev. A 65, 042327 (2002)

[11] G. Tóth, Phys. Rev. A 71, 010301(R) (2005)

[12] M. R. Dowling, A. C. Doherty and S. D. Barlett, Phys. Rev. A 70, 062113 (2004).

[13] Č. Brukner, V. Vedral and A. Zeilinger, Phys. Rev. A 73, 012110 (2006).

[14] M. Wieśniak, V. Vedral and Č. Brukner, New Journal of Physics 7, 258 (2005).

[15] S. Ghosh, T. F. Rosenbaum, G. Aeppli and S. N. Coppersmith, Nature (London) 425, 48 (2003): V. Vedral. *ibid.* 425,28 (2003).

[16] I. Bose and A. Tribedi, Phys. Rev. A 72, 022314 (2005).

[17] T. Veŕtesi and E. Bene, Phys. Rev. B 73, 134404 (2006).

[18] J. T. Haraldsen, T. Barnes and J. L. Musfeldt, Phys. Rev. B 71, 064403 (2005).

[19] M. U.-Kartin, S.-J. Hwu and J. A. Clayhold, Inorg. Chem. 2003, 42, 2405-2409; J. A. Clayhold, Research on Novel Magnetic Solids, Magnetic Materials, Miami University.

[20] J. Strečka et al., J. Phys. Chem. Solids 66, 1828 (2005).

[21] V. V. Mikhailov, J. Phys. A : Math. Gen. 10, 147 (1977).

[22] X. Hao and S. Zhu, Phys. Rev. A 72, 042306 (2005).

[23] I. Bose and E. Chattopadhyay, Phys. Rev. A 66, 062320 (2002).

[24] L.-A Wu, M. S. Sarandy and D. A. Lidar, Phys. Rev. Lett. 93, 250404 (2004).

[25] F. C. Alcaraz, A. Saguia and M. S. Sarandy, Phys. Rev. A 70, 032333 (2004).

[26] J. Vidal, R. Mosseri and J. Dukelsky, Phys. Rev. A 69, 054101 (2004).

[27] I. Bose, Current Science 88, 62 (2005).

[28] M. Oshikawa, M. Yamanaka and I. Affleck, Phys. Rev. Lett. 78, 1984 (1997).

[29] H. Kagemaya et al., Phys. Rev. Lett. 82, 3168 (1999); K. Onizuka et al., J. Phys. Soc. Jpn. 69, 1016 (2004); K. Kodama et al., Science 298, 395 (2002).

Appendix A: Eigenvalues and eigenvectors of linear chain tetramer

The Hamiltonian describing the linear chain tetramer is given in Eq. (7). The total spin of the tetramer is S^{tot}. The first index in the subscript of an eigenvector refers to the eigenvalue and the second to S_z^{tot}, the z-component of the total spin.

$S^{tot} = 2$:

$$E_1 = \left(\tfrac{1}{2} + \tfrac{\alpha}{4}\right) J \qquad (A1)$$

$$\begin{gathered} \psi_{1,2} = |\uparrow\uparrow\uparrow\uparrow\rangle \\ \psi_{1,1} = \tfrac{1}{2}\left(|\downarrow\uparrow\uparrow\uparrow\rangle + |\uparrow\downarrow\uparrow\uparrow\rangle + |\uparrow\uparrow\downarrow\uparrow\rangle + |\uparrow\uparrow\uparrow\downarrow\rangle\right) \\ \psi_{1,0} = \tfrac{1}{\sqrt{6}}\left(|\uparrow\uparrow\downarrow\downarrow\rangle + |\uparrow\downarrow\uparrow\downarrow\rangle + |\uparrow\downarrow\downarrow\uparrow\rangle + |\downarrow\uparrow\uparrow\downarrow\rangle + |\downarrow\uparrow\downarrow\uparrow\rangle + |\downarrow\downarrow\uparrow\uparrow\rangle\right) \\ \psi_{1,-1} = \tfrac{1}{2}\left(|\uparrow\downarrow\downarrow\downarrow\rangle + |\downarrow\uparrow\downarrow\downarrow\rangle + |\downarrow\downarrow\uparrow\downarrow\rangle + |\downarrow\downarrow\downarrow\uparrow\rangle\right) \\ \psi_{1,-2} = |\downarrow\downarrow\downarrow\downarrow\rangle \end{gathered} \qquad (A2)$$

$S^{tot} = 1$:

$$E_2 = (-\frac{1}{2} + \frac{\alpha}{4})J \qquad (A3)$$

$$\begin{gathered} \psi_{2,1} = \tfrac{1}{2}\left(|\downarrow\uparrow\uparrow\uparrow\rangle - |\uparrow\downarrow\uparrow\uparrow\rangle - |\uparrow\uparrow\downarrow\uparrow\rangle + |\uparrow\uparrow\uparrow\downarrow\rangle\right) \\ \psi_{2,-1} = \tfrac{1}{2}\left(|\downarrow\uparrow\uparrow\uparrow\rangle - |\uparrow\downarrow\uparrow\uparrow\rangle - |\uparrow\uparrow\downarrow\uparrow\rangle + |\uparrow\uparrow\uparrow\downarrow\rangle\right) \\ \psi_{2,0} = \tfrac{1}{\sqrt{6}}\left(|\uparrow\downarrow\downarrow\uparrow\rangle - |\downarrow\uparrow\uparrow\downarrow\rangle\right) \end{gathered} \qquad (A4)$$

$$E_3 = (-\frac{\alpha}{4} + \frac{1}{2}\sqrt{1+\alpha^2})J \qquad (A5)$$

$$\begin{gathered} \psi_{3,1} = \tfrac{1}{N_1}\left(|\downarrow\uparrow\uparrow\uparrow\rangle - |\uparrow\uparrow\uparrow\downarrow\rangle - \left(\alpha - \sqrt{1+\alpha^2}\right)\left(|\uparrow\downarrow\uparrow\uparrow\rangle - |\uparrow\uparrow\downarrow\uparrow\rangle\right)\right) \\ \psi_{3,-1} = \tfrac{1}{N_1}\left(|\uparrow\downarrow\downarrow\downarrow\rangle - |\downarrow\downarrow\downarrow\uparrow\rangle - \left(\alpha - \sqrt{1+\alpha^2}\right)\left(|\downarrow\uparrow\downarrow\downarrow\rangle - |\downarrow\downarrow\uparrow\downarrow\rangle\right)\right) \\ \psi_{3,0} = \tfrac{1}{N_2}\left(|\uparrow\uparrow\downarrow\downarrow\rangle - |\downarrow\downarrow\uparrow\uparrow\rangle - \left(\tfrac{1}{\alpha} - \sqrt{1+\tfrac{1}{\alpha^2}}\right)\left(|\uparrow\downarrow\uparrow\downarrow\rangle - |\downarrow\uparrow\downarrow\uparrow\rangle\right)\right) \end{gathered} \qquad (A6)$$

$$E_4 = (-\frac{\alpha}{4} - \frac{1}{2}\sqrt{1+\alpha^2}) \qquad (A7)$$

$$\begin{gathered} \psi_{4,1} = \tfrac{1}{N_3}\left(|\downarrow\uparrow\uparrow\uparrow\rangle - |\uparrow\uparrow\uparrow\downarrow\rangle - \left(\alpha + \sqrt{1+\alpha^2}\right)\left(|\uparrow\downarrow\uparrow\uparrow\rangle - |\uparrow\uparrow\downarrow\uparrow\rangle\right)\right) \\ \psi_{4,-1} = \tfrac{1}{N_3}\left(|\uparrow\downarrow\downarrow\downarrow\rangle - |\downarrow\downarrow\downarrow\uparrow\rangle - \left(\alpha + \sqrt{1+\alpha^2}\right)\left(|\downarrow\uparrow\downarrow\downarrow\rangle - |\downarrow\downarrow\uparrow\downarrow\rangle\right)\right) \\ \psi_{4,0} = \tfrac{1}{N_4}\left(|\uparrow\uparrow\downarrow\downarrow\rangle - |\downarrow\downarrow\uparrow\uparrow\rangle - \left(\tfrac{1}{\alpha} + \sqrt{1+\tfrac{1}{\alpha^2}}\right)\left(|\uparrow\downarrow\uparrow\downarrow\rangle - |\downarrow\uparrow\downarrow\uparrow\rangle\right)\right) \end{gathered} \qquad (A8)$$

$S^{tot} = 0$:

$$E_5 = \left\{ -\left(\frac{1}{2} + \frac{\alpha}{4}\right) + \sqrt{1 - \frac{\alpha}{2} + \frac{\alpha^2}{4}} \right\} J \qquad (A9)$$

$$\psi_{5,0} = \frac{1}{N_5} \left(a_1 \left|\uparrow\uparrow\downarrow\downarrow\right\rangle + b_1 \left|\uparrow\downarrow\uparrow\downarrow\right\rangle + c_1 \left|\uparrow\downarrow\downarrow\uparrow\right\rangle + d_1 \left|\downarrow\uparrow\uparrow\downarrow\right\rangle + e_1 \left|\downarrow\uparrow\downarrow\uparrow\right\rangle + f_1 \left|\downarrow\downarrow\uparrow\uparrow\right\rangle \right) \qquad (A10)$$

$$E_6 = \left\{ -\left(\frac{1}{2} + \frac{\alpha}{4}\right) - \sqrt{1 - \frac{\alpha}{2} + \frac{\alpha^2}{4}} \right\} J \qquad (A11)$$

$$\psi_{5,0} = \frac{1}{N_6} \left(a_2 \left|\uparrow\uparrow\downarrow\downarrow\right\rangle + b_2 \left|\uparrow\downarrow\uparrow\downarrow\right\rangle + c_2 \left|\uparrow\downarrow\downarrow\uparrow\right\rangle + d_2 \left|\downarrow\uparrow\uparrow\downarrow\right\rangle + e_2 \left|\downarrow\uparrow\downarrow\uparrow\right\rangle + f_2 \left|\downarrow\downarrow\uparrow\uparrow\right\rangle \right) \qquad (A12)$$

where $a_1 = f_1 = a_2 = f_2 = 1$, $b_1 = -\frac{2}{\alpha} + 2\sqrt{\frac{1}{4} - \frac{1}{2\alpha} + \frac{1}{\alpha^2}} = e_1$, $b_2 = -\frac{2}{\alpha} - 2\sqrt{\frac{1}{4} - \frac{1}{2\alpha} + \frac{1}{\alpha^2}} = e_2$, $c_1 = -1 + \frac{2}{\alpha} - 2\sqrt{\frac{1}{4} - \frac{1}{2\alpha} + \frac{1}{\alpha^2}} = d_1$, $c_2 = -1 + \frac{2}{\alpha} + 2\sqrt{\frac{1}{4} - \frac{1}{2\alpha} + \frac{1}{\alpha^2}} = d_2$
N_1, N_2, N_3, N_4, N_5 and N_6 are the appropriate normalization constants.

Appendix B: Eigenvalues and eigenvectors of the spin-1 dimer

The dimer Hamiltonian H_d is given by Eq. (21). The basis functions are represented as $|S_1^z, S_2^z\rangle$ with $S_1^z = \pm 1, 0$ and $S_2^z = \pm 1, 0$. The eigenstates and the eigenvalues are described by $\phi_{n,m}$ and $\lambda_{n,m}$ where 'n' and 'm' refer to the total spin S^{tot} of the dimer and its z-component respectively.

$S^{tot} = 2$:

$$\begin{gathered} \phi_{2,\pm 2} = |\pm 1, \pm 1\rangle \\ \lambda_{2,\pm 2} = \delta J + 2d \pm 2B \end{gathered} \qquad (B1)$$

$$\begin{gathered} \phi_{2,\pm 1} = \tfrac{1}{\sqrt{2}} \left(|\pm 1, 0\rangle + |0, \pm 1\rangle \right) \\ \lambda_{2,\pm 1} = J + d \pm B \end{gathered} \qquad (B2)$$

$$\begin{gathered} \phi_{2,0} = \tfrac{1}{2} \left(A_m \left|1, -1\right\rangle + \left|-1, 1\right\rangle \right) + \sqrt{2} A_p \left|0, 0\right\rangle \\ \lambda_{2,0} = -\tfrac{\delta J}{2} + d + R \end{gathered} \qquad (B3)$$

$S^{tot} = 1$:

$$\begin{gathered} \phi_{1,\pm 1} = \tfrac{1}{\sqrt{2}} \left(|\pm 1, 0\rangle - |0, \pm 1\rangle \right) \\ \lambda_{1,\pm 1} = -J + d \pm B \end{gathered} \qquad (B4)$$

$$\begin{array}{c} \phi_{1,0} = \frac{1}{\sqrt{2}} \left(|1,-1\rangle - |-1,1\rangle \right) \\ \lambda_{2,\pm 1} = -\delta J + 2d \end{array} \qquad (B5)$$

$S^{tot} = 0$:

$$\begin{array}{c} \phi_{0,0} = \frac{1}{2} \left(A_p \left(|1,-1\rangle + |-1,1\rangle \right) - \sqrt{2} A_m \left| 0,0 \right\rangle \right) \\ \lambda_{0,0} = -\frac{\delta J}{2} + d - R \end{array} \qquad (B6)$$

where

$$\begin{array}{c} R = \left[\left(\frac{\delta J}{2} - d \right)^2 + 2J^2 \right]^{\frac{1}{2}} \\ A_p = \left(\frac{R + \frac{\delta J}{2} - d}{R} \right)^{\frac{1}{2}} \\ A_m = \left(\frac{R - \frac{\delta J}{2} + d}{R} \right)^{\frac{1}{2}} \end{array} \qquad (B7)$$